Luminescent Heterometallic Branched Alkynyl Complexes of Rhenium(I)−Palladium(II): Potential Building Blocks for Heterometallic Metallodendrimers

Samuel Hung-Fai Chong, Sally Chan-Fung Lam, Vivian Wing-Wah Yam,*
Nianyong Zhu, and Kung-Kai Cheung

*Centre for Carbon-Rich Molecular and Nano-Scale Metal-Based Materials Research, and the
Department of Chemistry, The University of Hong Kong, Pokfulam Road,
Hong Kong, People's Republic of China*

Sofiane Fathallah, Karine Costuas, and Jean-François Halet*

*Laboratoire de Chimie du Solide et Inorganique Moléculaire, UMR 6511 CNRS, Université de
Rennes 1, Institut de Chimie de Rennes, F-35042 Rennes, France*

The photophysical and electrochemical behavior of a novel series of luminescent rhenium(I) complexes bearing a trialkynyl ligand, $[1,3\text{-}(HC\equiv C)_2\text{-}5\text{-}\{(N^\wedge N)(CO)_3ReC\equiv C\}C_6H_3]$ ($N^\wedge N$ = $^tBu_2bpy$ **1**, Me_2bpy **2**, bpy **3**), and their heterometallic branched complexes, $[1,3\text{-}\{Cl(PEt_3)_2PdC\equiv C\}_2\text{-}5\text{-}\{(N^\wedge N)(CO)_3ReC\equiv C\}C_6H_3]$ ($N^\wedge N$ = Me_2bpy **4**, bpy **5**), have been studied; the X-ray crystal structures of **2** and **5** have been determined. Density functional theory calculations have also been carried out in order to probe the bonding in these compounds.

Introduction

There is a constant search for organometallic dendrimers with unique and interesting properties that are inaccessible by their organic counterparts.[1] Multidimensional alkynyl ligands, such as 1,3,5-triethynylbenzene, are of particular interest for the construction of organometallic dendrimers due to their geometry and active coordination sites, which enable the extension of the core in three directions. Such three-dimensional hyperbranched polymers or dendrimers usually have a lower intrinsic viscosity and better solubility than the corresponding linear polymers with similar molecular weights. Currently, dendritic molecules have attracted much attention of numerous researchers because of their interesting electrochemical,[2] catalytic,[3] and energy transfer properties.[4] Indeed, the organometallic dendrimers are useful in building carbon-rich networks,[5] supramolecular polymetallic assemblies,[6] nanoarchitectures for materials science,[7] and fabricating nanoscale optical and electronic devices for nanotechnology.[4a,8] A

number of examples featuring this core unit have recently been reported. Stang and co-workers reported the synthesis of $[1,3,5\text{-}\{trans\text{-}I(Et_3P)_2Pt(C\equiv C)\}_3C_6H_3]$ and $[1,2,4,5\text{-}\{trans\text{-}I(Et_3P)_2Pt(C\equiv C)\}_4C_6H_2]$, which serve as versatile precursors to platinum-containing dendrimers.[9] Takahashi and co-workers reported the synthesis of a series of platinum-alkynyl dendrimers using this triethynylbenzene core as bridging ligand, and dendrimers containing up to 189 platinum atoms have also been synthesized.[10] Long and co-workers reported on a series of complexes featuring *trans*-[Ru(dppm)₂Cl], *trans*-[Os(dppm)₂Cl], or [Ru(η-C₅H₅)(PPh₃)₂] and ferrocenyl [(C₅H₅FeC₅H₄)] units unsymmetrically arranged around the periphery of a 1,3,5-triethynylbenzene core, the spectroscopic characterizations and electrochemical properties of which have also been studied in detail.[11] Although an increasing number of works that involve dendrimers with this trifunctional alkynyl core molecule

* To whom correspondence should be addressed. E-mail: wwyam@ hku.hk (V.W.-W.Y); halet@univ-rennes1.fr (J.-F.H).

(1) Newkome, G. R.; Moorefield, C. N.; Vögtle, F. *Dendritic Molecules: Concepts, Synthesis, Perspectives*, VCH: Weinheim, Germany, 1996. (b) Cuadrado, I.; Morán, M.; Casado, C. M.; Alonso, B.; Losada, J. *Coord. Chem. Rev.* **1999**, *193−195*, 395.

(2) Long, N. J.; Angela, A. J.; de Biani, F. F.; Zanello, P. *J. Chem. Soc., Dalton Trans.* **1998**, 2017.

(3) Köllner, C.; Pugin, B.; Togni, A. *J. Am. Chem. Soc.* **1998**, *120*, 10274.

(4) (a) Revadoss, C.; Bharathi, P.; Moore, J. S. *J. Am. Chem. Soc.* **1996**, *118*, 9635. (b) Hu, Q. S.; Pugh, V.; Sabat, M.; Pu, L. *J. Org. Chem.* **1999**, *64*, 7528.

(5) (a) Diederich, F. *Nature* **1994**, *369*, 149. (b) Diederich, F. *Modern Acetylene Chemistry*; VCH: Weinheim, 1995; p 443. (c) Faust, R.; Diederich, F.; Gramlich, V.; Seiler, P. *Chem. Eur. J.* **1995**, *1*, 111.

(6) (a) Venkataraman, D.; Lee, S.; Moore, J. S.; Zhang, P.; Hirsch, K. A.; Gardner, G. B. A.; Covey, C.; Prentice, C. L. *Chem. Mater.* **1996**, *8*, 2030. (b) Irwin, M. J.; Manojlovic-Muir, L.; Muir, K. W.; Puddephatt, R. J.; Yufit, D. S. *Chem. Commun.* **1997**, 219.

(7) (a) Schumm, J. S.; Pearson, D. L.; Tour, J. M. *Angew. Chem., Int. Ed. Engl.* **1994**, *33*, 1360. (b) Campagna, S.; Denti, G.; Serroni, S.; Juris, A.; Venturi, M.; Riceunto, V.; Balzani, V. *Chem. Eur. J.* **1995**, *1*, 211.

(8) (a) Xu, Z.; Kahr, M.; Walker, K. L.; Wilkins, C. L.; Moore, J. S. *J. Am. Chem. Soc.* **1994**, *116*, 4537. (b) Xu, Z.; Moore, J. S. *Angew. Chem., Int. Ed. Engl.* **1993**, *32*, 1354. (c) Devadoss, C.; Bharathi, P.; Moore, J. S. *Macromolecules* **1998**, *31*, 8091.

(9) Leininger, S.; Stang, P. J.; Huang, S. *Organometallics* **1998**, *17*, 3981.

(10) (a) Ohshiro, N.; Takei, F.; Onitsuka, K.; Takahashi, S. *J. Organomet. Chem.* **1998**, *569*, 195. (b) Onitsuka, K.; Fujimoto, M.; Ohshiro, N.; Takahashi, S. *Angew. Chem., Int. Ed.* **1999**, *38*, 689. (c) Onitsuka, K.; Shimizu, A.; Takahashi, S. *Chem. Commun.* **2003**, 280. (d) Ohshiro, N.; Takei, F.; Onitsuka, K.; Takahashi, S. *Chem. Lett.* **1996**, 871.

Scheme 1. Synthetic Scheme of the Heteronuclear Rhenium(I) Alkynyl Complexes[a]

1, R = ^{t}Bu

2, R = Me

3, R = H

4, R = Me

5, R = H
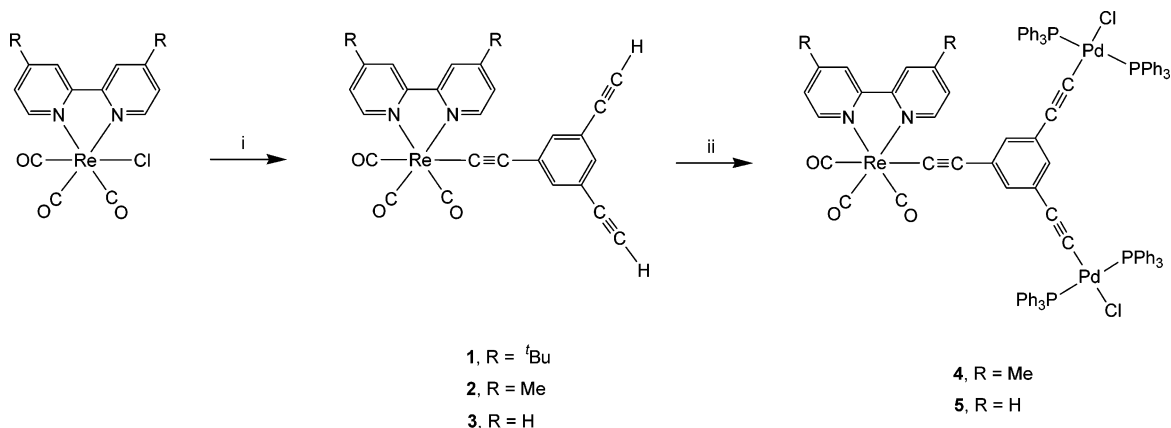
[a] Reaction conditions: (i) 1,3,5-(HC≡C)$_3$C$_6$H$_3$, AgOTf, Et$_3$N, THF; (ii) *trans*-[Pd(PEt$_3$)$_2$Cl$_2$], CuCl, Et$_3$N, THF.

are reported in the literature, hyperbranched molecules containing the tricarbonyl rhenium(I) diimine luminophore are still not known. Heterometallic dendrimeric molecules are also remarkably rare.[11] As an extension of our previous efforts on the study of luminescent branched Pd(II) and Pt(II) alkynyl complexes,[12] we have launched a program to study heterometallic branched alkynyl complexes based on the tricarbonyl rhenium(I) diimine core. Herein are reported the synthesis, structural characterization, and luminescence behavior of a series of Re(I) alkynyl precursors, [1,3-(HC≡C)$_2$-5-{(N^N)(CO)$_3$ReC≡C}C$_6$H$_3$] (N^N = ^{t}Bu$_2$bpy **1**, Me$_2$bpy **2**, bpy **3**), and their trinuclear branched Re(I)−Pd(II) mixed-metal alkynyl complexes, [1,3-{Cl(PEt$_3$)$_2$PdC≡C}$_2$-5-{(N^N)(CO)$_3$ReC≡C}C$_6$H$_3$] (N^N = Me$_2$bpy **4**, bpy **5**) (Scheme 1). DFT calculations have also been carried out on selected metal complexes in order to probe the bonding in this kind of compound.

Experimental Section

Materials and Reagents. [Re(CO)$_5$Cl] was obtained from Strem Chemicals, Inc. 2,2′-Bipyridine (bpy) and 4,4′-dimethyl-2,2′-bipyridine (Me$_2$bpy) were obtained from Aldrich Chemical Co. 4,4′-Di-*tert*-butyl-2,2′-bipyridine (^{t}Bu$_2$bpy) was prepared by a slight modification of the reported procedure.[13] Triethylamine was purchased from Lancaster Synthesis Ltd. Silver trifluoromethanesulfonate and copper(I) chloride were purchased from Aldrich Chemical Co. (1,3,5-(HC≡C)$_3$C$_6$H$_3$),[10d] [Re(CO)$_3$-(^{t}Bu$_2$bpy)Cl],[14] [Re(CO)$_3$(Me$_2$bpy)Cl],[15] [Re(CO)$_3$(bpy)Cl],[15] and *trans*-[Pd(PEt$_3$)$_2$Cl$_2$][16] were synthesized according to the literature procedures. All solvents were purified and distilled using standard procedures before use.[17] All other reagents were of analytical grade and were used as received.

(11) Long, N. J.; Martin, A. J.; White, A. J. P.; Williams, D. J.; Fontani, M.; Laschi, F.; Zanello, P. *J. Chem. Soc., Dalton Trans.* **2000**, 3387.

(12) (a) Yam, V. W. W.; Zhang, L.; Tao, C. H.; Wong, K. M. C.; Cheung, K. K. *J. Chem. Soc., Dalton Trans.* **2001**, 1111. (b) Yam, V. W. W.; Tao, C. H.; Zhang, L.; Wong, K. M. C.; Cheung, K. K. *Organometallics* **2001**, *20*, 453.

(13) Hadda, T. B.; Bozec, H. L. *Polyhedron* **1988**, *7*, 75.

(14) Yam, V. W. W.; Lau, V. C. Y.; Cheung, K. K. *Organometallics* **1995**, *14*, 2749.

(15) (a) Caspar, J. V.; Sullivan, B. P.; Meyer, T. J. *Inorg. Chem.* **1984**, *23*, 2104. (b) Sullivan, B. P.; Meyer, T. J. *J. Chem. Soc., Chem. Commun.* **1984**, 403.

(16) Okano, T.; Iwahara, M.; Konish, H.; Kiji, J. *J. Organomet. Chem.* **1988**, *346*, 267.

(17) Perrin, D. D.; Armarego, W. L. F. *Purification of Laboratory Chemicals*, 3rd ed.; Pergamon: Oxford, U.K., 1988.

Syntheses of Re(I) Alkynyl Precursors and Re(I)−Pd-(II) Mixed-Metal Alkynyl Complexes. All reactions were performed under anaerobic and anhydrous conditions using standard Schlenk techniques under an inert atmosphere of nitrogen.

[1,3-(HC≡C)$_2$-5-{(^{t}Bu$_2$bpy)(CO)$_3$ReC≡C}C$_6$H$_3$] (1). A mixture of [Re(CO)$_3$(^{t}Bu$_2$bpy)Cl] (100 mg, 0.17 mmol), Et$_3$N (52 mg, 0.51 mmol), AgOTf (48 mg, 0.19 mmol), and 1,3,5-(HC≡C)$_3$C$_6$H$_3$ (26 mg, 0.17 mmol) in THF (70 mL) was allowed to reflux under an inert atmosphere of nitrogen in the dark for 24 h. After cooling to room temperature, the dark brown suspension was filtered and the orange filtrate was reduced in volume under reduced pressure. The residue was then purified by column chromatography on silica gel using dichloromethane−petroleum ether (bp 40−60 °C) (4:1 v/v) as the eluent. After removal of the first band, which contains the unreacted 1,3,5-triethynylbenzene, the second band was collected, which gave the desired product. Subsequent recrystallization from vapor diffusion of diethyl ether into a dichloromethane solution of **1** gave orange crystals. Yield: 41 mg, 35%. ^{1}H NMR (300 MHz, acetone-d_6, 298 K, relative to Me$_4$-Si): δ 1.40 (s, 18H, ^{t}Bu), 3.40 (s, 2H, C≡CH), 6.90 (d, 2H, J = 1.5 Hz, 4- and 6-H on C$_6$H$_3$), 7.10 (t, 1H, J = 1.5 Hz, 2-H on C$_6$H$_3$), 7.80 (dd, 2H, J = 2.0 and 5.9 Hz, 5- and 5′-bipyridyl H's), 8.70 (d, 2H, J = 2.0 Hz, 3- and 3′-bipyridyl H's), 9.00 (d, 2H, J = 5.9 Hz, 6- and 6′-bipyridyl H's). Positive FAB-MS: ion clusters at m/z 690 {M}$^+$, 662 {M − CO}$^+$, 539 {M − [1,3-(HC≡C)$_2$-5-{C≡C}C$_6$H$_3$]}$^+$. IR (Nujol mull on KBr disk, ν/cm^{-1}): 2120 (w), 2107 (w), 2088 (m) ν(C≡C); 2004 (s), 1914 (s), 1888 (s) ν(C≡O). Anal. Found: C 57.93, H 4.55, N 3.86. Calcd for [1,3-(HC≡C)$_2$-5-{(^{t}Bu$_2$bpy)(CO)$_3$ReC≡C}C$_6$H$_3$]·1/2THF: C 58.20, H 4.46, N 3.90.

[1,3-(HC≡C)$_2$-5-{(Me$_2$bpy)(CO)$_3$ReC≡C}C$_6$H$_3$] (2). The procedure was similar to that described for the preparation of **1**, except [Re(CO)$_3$(Me$_2$bpy)Cl] (83 mg, 0.17 mmol) was used in place of [Re(CO)$_3$(^{t}Bu$_2$bpy)Cl] to give orange crystals of **2**. Yield: 41 mg, 30%. ^{1}H NMR (300 MHz, acetone-d_6, 298 K, relative to Me$_4$Si): δ 2.50 (s, 6H, −Me), 3.40 (s, 2H, C≡CH), 6.90 (d, 2H, J = 1.5 Hz, 4- and 6-H on C$_6$H$_3$), 7.10 (t, 1H, J = 1.5 Hz, 2-H on C$_6$H$_3$), 7.60 (dd, 2H, J = 1.9 and 5.9 Hz, 5- and 5′-bipyridyl H's), 8.60 (d, 2H, J = 1.9 Hz, 3- and 3′-bipyridyl H's), 8.80 (d, 2H, J = 5.9 Hz, 6- and 6′-bipyridyl H's). Positive FAB-MS: ion clusters at m/z 605 {M}$^+$, 576 {M − CO}$^+$, 455 {M − [1,3-(HC≡C)$_2$-5-{C≡C}C$_6$H$_3$]}$^+$. IR (Nujol mull on KBr disk, ν/cm^{-1}): 2120 (w), 2107(w), 2087 (m) ν(C≡C); 2004 (s), 1914 (s), 1882 (s) ν(C≡O). Anal. Found: C 52.17, H 3.06, N 4.51. Calcd for [1,3-(HC≡C)$_2$-5-{(Me$_2$bpy)(CO)$_3$ReC≡C}C$_6$H$_3$]: C 52.13, H 2.91, N 4.29.

[1,3-(HC≡C)$_2$-5-{(bpy)(CO)$_3$ReC≡C}C$_6$H$_3$] (3). The procedure was similar to that described for the preparation of **1**, except [Re(CO)$_3$(bpy)Cl] (79 mg, 0.17 mmol) was used in place

of [Re(CO)$_3$(^{t}Bu$_2$bpy)Cl] to give orange crystals of **3**. Yield: 39 mg, 32%. ^{1}H NMR (300 MHz, acetone-d_6, 298 K, relative to Me$_4$Si): δ 3.40 (s, 2H, C≡CH), 6.80 (d, 2H, J = 1.5 Hz, 4- and 6-H on C$_6$H$_3$), 7.10 (t, 1H, J = 1.5 Hz, 2-H on C$_6$H$_3$), 7.80 (t, 2H, J = 6.1 Hz, 4- and 4′-bipyridyl H's), 8.30 (t, 2H, J = 7.9 Hz, 5- and 5′-bipyridyl H's), 8.70 (d, 2H, J = 8.2 Hz, 3- and 3′-bipyridyl H's), 9.20 (d, 2H, J = 5.3 Hz, 6- and 6′-bipyridyl H's). Positive FAB-MS: ion clusters at m/z 578 {M}$^+$, 550 {M − CO}$^+$, 427 {M − [1,3-(HC≡C)$_2$-5-{C≡C}C$_6$H$_3$]}$^+$. IR (Nujol mull on KBr disk, ν/cm^{-1}): 2120 (w), 2108 (w), 2077 (m) ν(C≡C); 2011 (s), 1914 (s), 1883 (s) ν(C≡O). Anal. Found: C 51.69, H 1.91, N 4.53. Calcd for [1,3-(HC≡C)$_2$-5-{(bpy)(CO)$_3$ReC≡C}C$_6$H$_3$]·^{1}/$_{10}$CH$_2$Cl$_2$: C 51.61, H 2.27, N 4.79.

[1,3-{Cl(PEt$_3$)$_2$PdC≡C}$_2$-5-{(Me$_2$bpy)(CO)$_3$ReC≡C}C$_6$H$_3$] (4). To a suspension of *trans*-[Pd(PEt$_3$)$_2$Cl$_2$] (211 mg, 0.51 mmol), CuCl (0.50 mg, 0.0051 mmol), and Et$_3$N (52 mg, 0.51 mmol) in THF (20 mL) was added dropwise a solution of **2** (103 mg, 0.17 mmol) in THF (20 mL). The reaction mixture was allowed to stir at room temperature in an inert atmosphere of nitrogen for 2 h. The orange suspension was filtered, and the orange filtrate was reduced in volume under reduced pressure. The residue was then purified by column chromatography on silica gel using dichloromethane as eluent. After removal of the first band, which contains unreacted **2**, ethyl acetate was used to elute out the second band, which contains **4** as the desired product. Subsequent recrystallization from vapor diffusion of diethyl ether into a dichloromethane solution of **4** gave orange crystals. Yield: 62 mg, 27%. ^{1}H NMR (300 MHz, acetone-d_6, 298 K, relative to Me$_4$Si): δ 1.10 (m, 36H, −CH$_3$ on ethyl groups), 1.80 (m, 24H, −CH$_2$ on ethyl groups), 2.50 (s, 6H, methyl H's on Me$_2$bpy), 6.50 (d, 2H, J = 1.4 Hz, 4- and 6-H on C$_6$H$_3$), 6.70 (t, 1H, J = 1.4 Hz, 2-H on C$_6$H$_3$), 7.50 (dd, 2H, J = 1.9 and 5.7 Hz, 5- and 5′-bipyridyl H's), 8.50 (d, 2H, J = 1.9 Hz, 3- and 3′-bipyridyl H's), 8.80 (d, 2H, J = 5.7 Hz, 6- and 6′-bipyridyl H's). Positive FAB-MS: ion clusters at m/z 1360 {M}$^+$, 1324 {M − CO}$^+$, 1098 {M − Pd(PEt$_3$)$_2$Cl}$^+$, 455 {M − [1,3-{Cl(PEt$_3$)$_2$PdC≡C}$_2$-5-{C≡C}C$_6$H$_3$]}$^+$. IR (Nujol mull on KBr disk, ν/cm^{-1}): 2102 (m, br) ν(C≡C); 2005 (s), 1910 (s), 1895 (s) ν(C≡O). Anal. Found: C 46.19, H 5.81, N 1.96. Calcd for [1,3-{Cl(PEt$_3$)$_2$PdC≡C}$_2$-5-{(Me$_2$bpy)(CO)$_3$ReC≡C}-C$_6$H$_3$]·C$_4$H$_8$O: C 46.02, H 5.81, N 1.98.

[1,3-{Cl(PEt$_3$)$_2$PdC≡C}$_2$-5-{(bpy)(CO)$_3$ReC≡C}C$_6$H$_3$] (5). The procedure was similar to that described for the preparation of **4**, except [1,3-(HC≡C)$_2$-5-{(bpy)(CO)$_3$ReC≡C}C$_6$H$_3$] (98 mg, 0.17 mmol) was used in place of [1,3-(HC≡C)$_2$-5-{(Me$_2$-bpy)(CO)$_3$ReC≡C}C$_6$H$_3$]. Subsequent recrystallization from dichloromethane−methanol afforded **5** as an orange solid. Single crystals of **5** were obtained by recrystallization from dichloromethane−n-hexane. Yield: 66 mg, 29%. ^{1}H NMR (300 MHz, acetone-d_6, 298 K, relative to Me$_4$Si): δ 1.10 (m, 36H, −CH$_3$ on ethyl groups), 1.80 (m, 24H, −CH$_2$ on ethyl groups), 6.50 (d, 2H, J = 1.4 Hz, 4- and 6-H on C$_6$H$_3$), 6.70 (t, 1H, J = 1.4 Hz, 2-H on C$_6$H$_3$), 7.70 (t, 2H, J = 5.6 Hz, 4- and 4′-bipyridyl H's), 8.20 (t, 2H, J = 7.9 Hz, 5- and 5′-bipyridyl H's), 8.60 (d, 2H, J = 8.2 Hz, 3- and 3′-bipyridyl H's), 9.10 (d, 2H, J = 4.7 Hz, 6- and 6′-bipyridyl H's). Positive FAB-MS: ion clusters at m/z 1331 {M}$^+$, 1247 {M − 3CO}$^+$, 427 {M − [1,3-{Cl(PEt$_3$)$_2$PdC≡C}$_2$-5-{C≡C}C$_6$H$_3$]}$^+$. IR (Nujol mull on KBr disk, ν/cm^{-1}): 2120 (m), 2104 (m, br) ν(C≡C); 2005 (s), 1912 (s), 1891 (s) ν(C≡O). Anal. Found: C 44.84, H 5.49, N 2.05. Calcd for [1,3-{Cl(PEt$_3$)$_2$PdC≡C}$_2$-5-{(bpy)(CO)$_3$ReC≡C}C$_6$H$_3$]: C 44.60, H 5.55, N 1.92.

Physical Measurements and Instrumentation. UV−visible spectra were obtained on a Hewlett-Packard 8452A diode array spectrophotometer, IR spectra as Nujol mulls on a Bio-Rad FTS-7 Fourier transform infrared spectrophotometer (4000−400 cm^{-1}), and steady-state excitation and emission spectra on a Spex Fluorolog-2 Model F 111 fluorescence spectrofluorometer equipped with a Hamamatsu R-928 photomultiplier tube. Low-temperature (77 K) spectra were

recorded by using an optical Dewar sample holder. ^{1}H NMR spectra were recorded on a Bruker DPX-300 (300 MHz) Fourier transform NMR spectrometer with chemical shifts recorded relative to Me$_4$Si. Positive-ion FAB mass spectra were recorded on a Finnigan MAT95 mass spectrometer. Elemental analyses for the metal complexes were performed on the Carlo Erba 1106 elemental analyzer at the Institute of Chemistry, Chinese Academy of Sciences.

Emission lifetime measurements were performed using a conventional laser system. The excitation source was the 355 nm output (third harmonic) of a Spectra-Physics Quanta-Ray Q-switched GCR-150 pulsed Nd:YAG laser (10 Hz). Luminescence decay signals were recorded on a Tektronix Model TDS-620A (500 MHz, 2GS/s) digital oscilloscope and analyzed using a program for exponential fits. All solutions for photophysical studies were degassed on a high-vacuum line in a two-compartment cell consisting of a 10 mL Pyrex bulb and a 1-cm path length quartz cuvette and sealed from the atmosphere by a Bibby Rotaflo HP6 Teflon stopper. The solutions were subject to at least four freeze−pump−thaw cycles.

Cyclic voltammetric measurements were performed by using a CH Instruments, Inc. Model CHI 620 electrochemical analyzer interfaced to a personal computer. The electrolytic cell used was a conventional two-compartment cell. The salt bridge of the reference electrode was separated from the working electrode compartment by a Vycor glass. A Ag/AgNO$_3$ (0.1 M in CH$_3$CN) reference electrode was used. The ferrocenium−ferrocene couple was used as the internal standard in the electrochemical measurements in acetonitrile (0.1 M ^{n}Bu$_4$-NPF$_6$).[18] The working electrode was a glassy carbon (Atomergic Chemetals V25) electrode with a platinum foil acting as the counter electrode.

DFT Calculations. Calculations were carried out at the BP86 level of density functional theory (DFT) as implemented in the Gaussian-98 suite of programs.[19] The complexes [1,3-(HC≡C)$_2$-5-{(bpy)(CO)$_3$ReC≡C}C$_6$H$_3$] (**3**) and the hydrogen-substituted model complex [1,3-{Cl(PH$_3$)$_2$PdC≡C}$_2$-5-{(bpy)-(CO)$_3$ReC≡C}C$_6$H$_3$] (**5-H**), used to mimic compounds **1**−**3** and **4**−**5**, respectively, were fully optimized with the LANL2DZ basis set and an additional set of polarization functions as introduced by Hay and Wadt, without any symmetry constraint.[20] In all cases the structural arrangements obtained were all very close to C_s symmetry. Therefore, C_s symmetry was considered.

Crystal Structure Determination. Crystals of **2** were obtained by recrystallization from vapor diffusion of diethyl ether into a dichloromethane solution of **2**. [2(C$_{27}$H$_{17}$N$_2$O$_3$Re)·C$_5$H$_{12}$]; M_r = 1279.45, triclinic, space group $P\bar{1}$ (No. 2), a = 13.025(3) Å, b = 14.515(5) Å, c = 16.632(5) Å, α = 113.00(3)°, β = 101.75(3)°, γ = 106.82(3)°, V = 2585(2) Å^3, Z = 2, D_c = 1.643 g cm^{-3}, μ(Mo Kα) = 48.98 cm^{-1}, F(000) = 1252. An orange crystal of dimensions 0.30 × 0.10 × 0.07 mm mounted on a glass fiber was used for data collection at 28 °C on a

(18) Gagne, R. R.; Koval, C. A.; Lisensky, G. C. *Inorg. Chem.* **1980**, *19*, 2854.

(19) Frisch, M. J. T., G. W.; Schlegel, H. B.; Scuseria, G. E.; Robb, M. A.; Cheeseman, J. R.; Zakrzewski, V. G.; Montgomery, J. A., Jr.; Stratmann, R. E.; Burant, J. C.; Dapprich, S.; Millam, J. M.; Daniels, A. D.; Kudin, K. N.; Strain, M. C.; Farkas, O.; Tomasi, J.; Barone, V.; Cossi, M.; Cammi, R.; Mennucci, B.; Pomelli, C.; Adamo, C.; Clifford, S.; Ochterski, J.; Petersson, G. A.; Ayala, P. Y.; Cui, Q.; Morokuma, K.; Malick, D. K.; Rabuck, A. D.; Raghavachari, K.; Foresman, J. B.; Cioslowski, J.; Ortiz, J. V.; Stefanov, B. B.; Liu, G.; Liashenko, A.; Piskorz, P.; Komaromi, I.; Gomperts, R.; Martin, R. L.; Fox, D. J.; Keith, T.; Al-Laham, M. A.; Peng, C. Y.; Nanayakkara, A.; Gonzalez, C.; Challacombe, M.; Gill, P. M. W.; Johnson, B.; Chen, W.; Wong, M. W.; Andres, J. L.; Gonzalez, C.; Head-Gordon, M.; Replogle, E. S.; Pople, J. A. *Gaussian98*, revision A.5; Gaussian, Inc.: Pittsburgh, PA, 1998.

(20) (a) Hay, P. J.; Wadt, W. R. *J. Chem. Phys.* **1985**, *82*, 299. (b) Dunning, T. H., Jr.; Hay, P. J. In *Modern Theoretical Chemistry*; Schaefer, H. F., III, Ed.; Plenum: New York, 1976. (c) Huzinaga, S. A., J.; Klobukowski, M.; Radzio-Andzelm, E.; Sakai, Y.; Tatewaki, H. *Gaussian Basis Sets for Molecular Calculations*; Elsevier: Amsterdam, 1984.

Table 1. Crystal and Structure Determination Data for Complexes 2 and 5

	2	**5**
molecular formula	$[2(C_{27}H_{17}N_2O_3Re)\cdot C_5H_{12}]$	$[ReC_{50}H_{77}N_2O_5P_4Cl_2Pd_2]$
fw	1279.45	1379.92
crystal system	triclinic	monoclinic
space group	$P\bar{1}$ (No. 2)	$C2/c$ (No. 15)
a, Å	13.025(3)	48.412(9)
b, Å	14.515(5)	8.390(2)
c, Å	16.632(5)	31.512(6)
α, deg	113.00(3)	90
β, deg	101.75(3)	102.52(3)
γ, deg	106.82(3)	90
V, Å^3	2585(2)	12495(4)
Z	2	8
μ, cm^{-1}	48.98	27.30
T, K	301	293
diffractometer	Rigaku AFC7R	MAR
cryst dimens, mm	$0.30 \times 0.10 \times 0.07$	$0.40 \times 0.10 \times 0.04$
λ/Å (graphite monochromated, Mo Kα)	0.71073	0.7103
R	0.034[a]	0.0516[b]
wR	0.050[a]	0.1452[b]
no. of data collected	9507	25006
no. of unique data	9117	8771
R_{int}	0.020	0.0383
no. of data used in refinement, m	6962	8771
no. of parameters refined, p	615	477

[a] $w = 4F_o^2/\sigma^2(F_o)^2$, where $\sigma^2(F_o)^2 = [\sigma^2(I) + (0.40F_o^2)^2]$ with $I > 3\sigma(I)$. [b] $w = 1/[\sigma^2(F_o^2) + (aP)^2 + bP]$, where $P = [2F_c^2 + \text{Max}(F_0^2,0)]/3$ with $I > 2\sigma(I)$.

Rigaku AFC7R diffractometer with graphite-monochromatized Mo Kα radiation (λ = 0.71073 Å) using $\omega-2\theta$ scans with ω-scan angle (0.73 + 0.35 tan θ)° at a scan speed of 8.0 deg min^{-1} (up to 6 scans for reflections with $I < 15\sigma(I)$). Unit-cell dimensions were determined on the basis of the setting angles of 25 reflections in the 2θ range of 41.7−43.5°. Intensity data (in the range of $2\theta_{max} = 50°$; h: −15 to 14; k: 0 to 17; l: −19 to 18 and three standard reflections measured after every 300 reflections showed decay of 7.86%) were corrected for decay and for Lorentz and polarization effects, and empirical absorption corrections based on the ψ-scan of five strong reflections (minimum and maximum transmission factors 0.252 and 1.000). A total of 9507 reflections were measured, of which 9117 were unique and R_{int} = 0.020. 6962 reflections with $I > 3\sigma(I)$ were considered observed and used in the structural analysis. The space group was determined on the basis of a statistical analysis of intensity distribution, and the successful refinement of the structure was solved by Patterson methods and expanded by Fourier methods (PATTY)[21] and refined by full-matrix least-squares using the software package TeXsan[22] on a Silicon Graphics Indy computer. One crystallographic asymmetric unit consists of two independent complex molecules and one *n*-pentane molecule. In the least-squares refinement, all 66 non-H atoms of the complex molecules were refined anisotropically, the five C atoms of the solvent molecule were refined isotropically, and 46 H atoms at calculated positions with thermal parameters equal to 1.3 times that of the attached C atoms were not refined. Convergence for 615 variable parameters by least-squares refinement F with $w = 4F_o^2/\sigma^2(F_o^2)$, where $\sigma^2(F_o^2) = [\sigma^2(I) + (0.040\ F_o^2)^2]$ for 6962 reflections with $I > 3\sigma(I)$, was reached at $R = 0.034$ and $wR = 0.050$ with a goodness-of-fit of 1.74. $(\Delta/\sigma)_{max} = 0.04$ except for the C atoms of the solvent molecule. The final difference Fourier map was featureless, with maximum positive and negative peaks of 1.38 and 0.74 e Å^{-3}, respectively. Crystal and structure determination data for **2** are summarized in Table 1. The final agreement factors for **2** are given in Table 1. Selected bond distances and angles are summarized in Table

(21) Beurskens, P. T.; Admiraal, G.; Beurskens, G.; Bosman, W. P.; Garcia-Granda, S.; Gould, R. O.; Smits, J. M. M.; Smykalla, C. *The DIRDIF program system*; Technical Report of the Crystallography Laboratory; University of Nijmegen: The Netherlands, 1992.
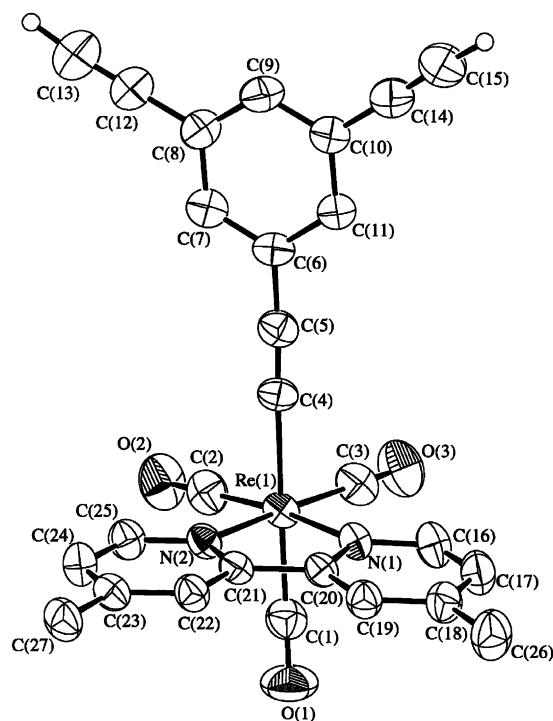(22) *TeXsan, Crystal Structure Analysis Package*; Molecular Structure Corporation: The Woodlands, TX, 1985 & 1992.

Table 2. Selected Bond Distances (Å) and Bond Angles (deg) for 2 and 5, with Estimated Standard Deviations (esd's) Given in Parentheses

2			
Re(1)−N(1)	2.194(5)	Re(1)−N(2)	2.193(5)
Re(1)−C(1)	1.954(8)	Re(1)−C(2)	1.904(8)
Re(1)−C(3)	1.921(8)	Re(1)−C(4)	2.161(7)
C(4)−C(5)	1.199(9)	C(12)−C(13)	1.16(1)
C(14)−C(15)	1.17(1)	C(1)−O(1)	1.133(9)
C(2)−O(2)	1.154(8)	C(3)−O(3)	1.134(9)
N(1)−Re(1)−N(2)	74.1(2)	N(1)−Re(1)−C(2)	172.2(2)
N(2)−Re(1)−C(3)	174.2(2)	C(1)−Re(1)−C(4)	174.6(3)
C(4)−C(5)−C(6)	176.9(7)	C(8)−C(12)−C(13)	178(1)
C(10)−C(14)−C(15)	177(1)	Re(1)−C(4)−C(5)	177.3(6)
5			
Re(1)−N(1)	2.138(6)	Re(1)−N(2)	2.171(8)
Re(1)−C(11)	1.934(12)	Re(1)−C(12)	1.887(12)
Re(1)−C(13)	1.895(13)	Re(1)−C(14)	2.143(10)
C(14)−C(15)	1.200(11)	C(22)−C(23)	1.207(12)
C(24)−C(25)	1.181(14)	C(11)−O(1)	1.159(13)
C(12)−O(2)	1.163(13)	C(13)−O(3)	1.152(12)
Pd(1)−C(23)	1.944(10)	Pd(2)−C(25)	1.924(11)
N(1)−Re(1)−N(2)	74.7(3)	C(13)−Re(1)−N(1)	172.5(4)
C(12)−Re(1)−N(2)	171.6(5)	C(11)−Re(1)−C(14)	174.2(5)
C(14)−C(15)−C(16)	175.8(10)	C(23)−C(22)−C(18)	176.4(10)
C(25)−C(24)−C(20)	177.0(11)	C(15)−C(14)−Re(1)	170.7(8)
P(1)−Pd(1)−Cl(1)	89.28(11)	P(2)−Pd(1)−Cl(1)	94.71(11)
P(3)−Pd(2)−Cl(2)	88.8(2)	P(4)−Pd(2)−Cl(2)	90.9(2)
P(3')−Pd(2)−Cl(2)	91.89(19)	P(4')−Pd(2)−Cl(2)	91.83(19)

2. The atomic coordinates and thermal parameters are given as Supporting Information.

Crystals of **5** were obtained by recrystallization from dichloromethane−*n*-hexane. [C$_{50}$H$_{77}$Cl$_2$N$_2$O$_5$P$_4$Pd$_2$Re]: M_r = 1379.92, monoclinic, space group $C2/c$ (No. 15), a = 48.412(9) Å, b = 8.390(2) Å, c = 31.512(6) Å, β = 102.52(3)°, V = 12495(4) Å^3, Z = 8, D_c = 1.467 g cm^{-3}, μ(Mo Kα) = 2.730 mm^{-1}, $F(000)$ = 5536. An orange crystal of dimensions $0.40 \times 0.10 \times 0.04$ mm mounted on a glass fiber was used for data collection at 20 °C on a MAR diffractometer with a 300 nm image plate detector using graphite-monochromatized Mo Kα radiation (λ = 0.71073 Å). Data collection was made with 2° oscillation step of φ, 600 s exposure time, and scanner distance at 120 mm. Ninety images were collected. The images were interpreted and

intensities interpreted using the program DENZO.[23] A total of 25 006 reflections were measured, of which 8771 were unique and R_{int} = 0.0383; 5582 reflections with larger than $4\sigma(F_o)$ were considered observed and used in the structural analysis. The space group was determined on the basis of a statistical analysis of intensity distribution and the successful refinement of the structure. The structure was solved by direct methods employing the SIR-97 program[24] on a PC and refinement by full-matrix least-squares using the software package SHELXL-97[25] on a PC. One crystallographic asymmetric unit consists of one water and one methanol solvent molecule. Two P atoms of the triethylphosphine ligands on Pd(2) were distorted each into two positions, which were separated by 0.80 and 0.54 Å, respectively; the ethyl groups on them were also distorted. In the least-squares refinement, all non-H atoms of the complex molecules were refined anisotropically, and the distorted atoms and the atoms mentioned above were refined isotropically. H atoms were generated by the program SHELXL-97.[25] The positions of H atoms were calculated on the basis of a riding mode with thermal parameters equal to 1.2 times that of the associated C atoms and participated in the calculation of final R-indices. Convergence for 477 variable parameters by full-matrix least-squares refinement on F^2 with $(\Delta/\sigma)_{max}$ = 0.002 (av 0.001) was reached at R_1 = 0.0516 and wR_2 = 0.1452 with a goodness-of-fit of 0.946. The final difference Fourier map showed maximum rest peaks and holes of 0.991 and −0.761 e Å^{-3}, respectively. Crystal and structure determination data for **5** are summarized in Table 1. The final agreement factors for **5** are given in Table 1. Selected bond distances and angles are summarized in Table 2. The atomic coordinates and thermal parameters are given as Supporting Information.

Results and Discussion

Reaction of a mixture of [Re(CO)$_3$(N^N)Cl], Et$_3$N, AgOTf, and 1,3,5-(HC≡C)$_3$C$_6$H$_3$ in THF under reflux conditions in an inert atmosphere of nitrogen for 24 h afforded [1,3-(HC≡C)$_2$-5-{(N^N)(CO)$_3$ReC≡C}C$_6$H$_3$], isolated as orange crystals after purification by column chromatography on silica gel, followed by recrystallization from dichloromethane−diethyl ether. On the other hand, reaction of a mixture of [1,3-(HC≡C)$_2$-5-{(N^N)(CO)$_3$ReC≡C}C$_6$H$_3$], *trans*-[Pd(PEt$_3$)$_2$Cl$_2$], CuCl, and Et$_3$N in THF at room temperature in an inert atmosphere of nitrogen for 2 h afforded [1,3-{Cl(PEt$_3$)$_2$Pd-C≡C}$_2$-5-{(N^N)(CO)$_3$ReC≡C}C$_6$H$_3$], isolated as orange crystals after purification by column chromatography on silica gel, followed by subsequent recrystallization from dichloromethane−diethyl ether, with the exception of **5** from a dichloromethane−*n*-hexane mixture. Addition of the THF solution of [1,3-(HC≡C)$_2$-5-{(N^N)(CO)$_3$ReC≡C}C$_6$H$_3$] to the reaction mixture in a dropwise manner was required to avoid the self-coupling reaction of the rhenium(I) alkynyl complexes. The identities of **1−5** have been confirmed by satisfactory elemental analyses, ^{1}H NMR, IR, and positive FAB-MS, and for complexes **2** and **5** also by X-ray crystallography.

The ^{1}H NMR spectra of the mononuclear rhenium(I) complexes **1−3** revealed a singlet at δ 3.40 ppm, corresponding to the acetylenic protons, which disappeared upon coordination of the alkynyl units to the

(23) Otwinowski, Z.; Minor, W. In *Methods in Enzymology, Vol. 276: Macromolecular Crystallography, part A*; Carter C. W., Sweet, R. M., Jr., Eds.; Academic Press: New York, 1997; pp 307−326.

(24) Altomare, A.; Burla, M. C.; Camalli, M.; Cascarano, G.; Giacovazzo, C.; Guagliardi, A.; Moliterni, A. G. G.; Polidori, G.; Spagna, R. A new tool for crystal structure determination and refinement. *J. Appl. Crystallogr.* **1998**, *32*, 115.

(25) Sheldrick, G. M. *SHELX97, Programs for Crystal Structure Analysis* (Release 97-2); University of Goetingen: Germany, 1997.

Figure 1. Perspective drawing of **2** with the atomic numbering scheme. Hydrogen atoms on the bipyridyl and phenyl rings have been omitted for clarity. Thermal ellipsoids are shown at the 40% probability level.

Pd(II) centers in the heterometallic complexes **4** and **5**. The aryl protons on the 2,4,6-positions of the central phenylene ring were found to show an upfield shift upon the coordination of the alkynyl groups to Pd(II). Such an upfield shift in the C$_6$H$_3$ signals in **4** and **5** compared with that in **1−3** may be suggestive of the electron-richness of the Pd(PEt$_3$)$_2$Cl moieties, leading to a reduced electron donation from the alkynyl unit.

The IR spectra of **1−3** exhibit three weak to medium intensity bands at ca. 2120−2077 cm^{-1}, corresponding to the two a$_1$ and one b$_1$ IR-active ν(C≡C) modes of **1−3** assuming a C_{2v} microsymmetry of the core and characteristic of ν(C≡C) stretches in metal alkynyl complexes. The medium intensity band at ca. 2087−2077 cm^{-1} in **2** and **3** shows an obvious reduction in intensity upon coordination to the palladium(II) metal centers in the trinuclear mixed-metal complexes **4** and **5**. Attempts to locate this third IR-active band in **4** and **5** were not possible since it was too weak to be observed. However, a slight shift of the weak ν(C≡C) band at ca. 2107 cm^{-1} in **2** and **3** to ca. 2103 cm^{-1} in **4** and **5** was observed. This may be suggestive of some weak back π-donation from the electron-rich Pd centers to the alkynyl units, causing a slight weakening of the C≡C bond.
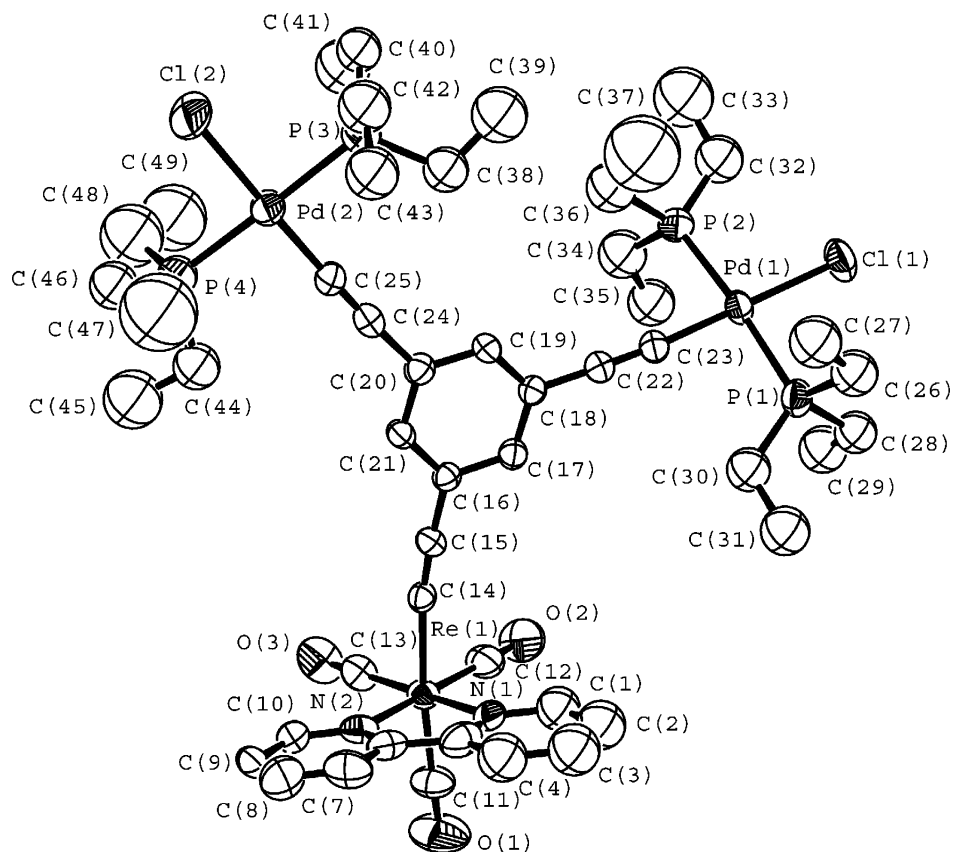
Figures 1 and 2 depict the perspective drawings of **2** and **5** with atomic numbering, respectively. Both structures show a slightly distorted octahedral geometry about Re with three carbonyl ligands arranged in a facial fashion. In both complexes, the N−Re−N bond angles of 74.1(2)° and 74.7(3)° for **2** and **5**, respectively, are less than 90°, as required by the bite distance exerted by the steric demand of the chelating bipyridine ligands.

The three C≡C bond lengths are 1.199(9), 1.16(1), and 1.17(1) Å for **2** and 1.200(11), 1.207(12), and 1.181(14)

Figure 2. Perspective drawing of **5** with the atomic numbering scheme. Hydrogen atoms on the bipyridyl, phenyl rings, and ethyl groups have been omitted for clarity. Thermal ellipsoids are shown at the 30% probability level.

Å for **5**, which are comparable to those found for other organometallic triethynylbenzene systems.[10a,b,d] The Re−C≡C unit for **2** is essentially linear, with a bond angle of 177.3(6)°, similar to those found for other related rhenium(I) alkynyl systems,[14,26] while the Re−C≡C bond in **5** shows a deviation from linearity with a bond angle of 170.7(8)°, which may be a result of the steric bulk of the two Pd(PEt₃)₂Cl moieties.

In complex **5**, both palladium centers show a slightly distorted square-planar coordination geometry, with the P−Pd−Cl bond angles in the range 88.8(2)−94.71(11)°. It is conceivable that a slight distortion from an ideal square-planar arrangement, which has also been observed in the crystal structure of *trans*-[PtCl(C≡CPh)(PEt₂Ph)₂],[27] could help to relieve steric interactions between the bulky groups. The coordination plane around Pd(1) forms an interplanar angle of 50.57° with the central phenylene ring, while that around Pd(2) are 10.50° and 26.48° due to the disorder of the two triethylphosphines on Pd(2).

The complex [1,3-(HC≡C)₂-5-{(bpy)(CO)₃ReC≡C}-C₆H₃] (**3**) and the hydrogen-substituted model complex [1,3-{Cl(PH₃)₂PdC≡C}₂-5-{(bpy)(CO)₃ReC≡C}C₆H₃] (**5-H**), used to mimic compounds **1−3** and **4−5**, respec-

tively, were optimized at the DFT level (see computational details). The pertinent computed distances are compared to the corresponding experimental distances of the crystallographically characterized complexes **2** and **5** in Figure 3. A rather good agreement is found. The largest deviation concerns the M−C bond distances computed, which are ca. 0.05−0.07 Å longer than that observed in **2** and **5**. This is mainly due to the fact that the relativistic effect is not completely taken into account in the calculations.[28] Although they are slightly longer overall, the computed C−C separations in the organic spacer are in a good agreement with the corresponding experimental values, which were measured with rather large uncertainties. They fall in the range of C−C distances generally measured experimentally for this kind of complex.[10a,b,d] The angles are reproduced at high accuracy, with deviations of less than 1°, except for the Re−C_α−C_β angle, which deviates in both **3** and **5-H** by 7° from the experimental values (178.6 and 180.0 vs 177.3(6)° in **2** and 170.7(8)° in **5**). The Pd environment in model **5-H** is nearly ideally square-planar with a P−Pd−Cl angle of 89°. Thus, the slight distortion observed experimentally in **5** can be unambiguously attributed to steric interactions. The computed dihedral angle between the central phenyl ring and the plane formed by the palladium and the phosphorus atoms is 45°. The corresponding experimental values are 51° around Pd(1) and 10° and 26° around Pd(2). This suggests that the bulky ligands present in

(26) (a) Yam, V. W. W.; Lau, V. C. Y.; Cheung, K. K. *Organometallics* **1996**, *15*, 1740. (b) Yam, V. W. W.; Chong, S. H. F.; Cheung, K. K. *Chem. Commun.* **1998**, 2121. (c) Yam, V. W. W.; Lo, K. K. W.; Wong, K. M. C. *J. Organomet. Chem.* **1999**, *578*, 3. (d) Yam, V. W. W.; Chong, S. H. F.; Ko, C. C.; Cheung, K. K. *Organometallics* **2000**, *19*, 5092. (e) Yam, V. W. W. *Chem. Commun.* **2001**, 789. (f) Yam, V. W. W.; Wong, K. M. C.; Chong, S. H. F.; Lau, V. C. Y.; Lam, S. C. F.; Zhang, L.; Cheung, K. K. *J. Organomet. Chem.* **2003**, *670*, 205.
(27) Cardin, C. J.; Cardin, D. J.; Lappart, M. F. K.; Muir, W. *J. Chem. Soc., Dalton Trans.* **1978**, 46.

(28) Koch, W.; Holthausen M. C. *A Chemist's Guide to Density Functional Theory*; Wiley-VCH: Weinheim, Germany, 2000.
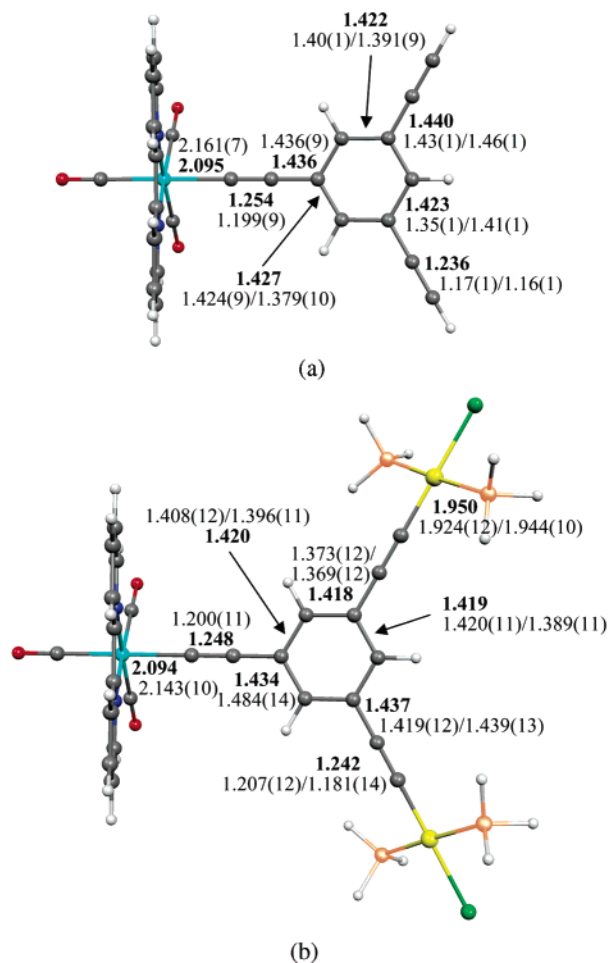
Figure 3. Pertinent computed distances (in bold) for complex **3** (a) and the hydrogen-substituted model complex **5-H** (b). Experimental distances measured for **2** and **5** are given for comparison, respectively.

5 prevent the structure from adopting a more symmetrical arrangement.

A comparison of the computed geometries of **3** and **5-H** indicates a slight shortening of the C≡C distance of the alkynyl unit bound to Re by 0.006 Å upon going from **3** to **5-H**. On the other hand, a slight lengthening of the same amount is computed for the C≡C distance of the alkynyl units bound to Pd in **5-H** with respect to the corresponding alkynyls in **3**. It is conceivable that some weak back π-donation from the electron-rich Pd centers to the alkynyl units is at work in **5-H**. Despite rather high uncertainties in the distances measured experimentally for **2** and **5**, the slight shift of the ν(C≡C) stretch to lower frequency upon coordination to palladium is also supportive of this point.

The DFT molecular orbital (MO) diagrams of complex **3** and the hydrogen-substituted model complex **5-H** are compared in Figure 4. A large HOMO−LUMO gap (1.13 eV) is computed for **3**. The HOMO and HOMO−1 orbitals of **3** show an important contribution of the alkynyl unit bound to Re and to a lesser extent of the rhenium atom. They result from antibonding interactions between dπ FMOs of the rhenium unit and in-plane and out-of-plane orbitals of the triethynylbenzene moiety. This is a common feature for organometallic complexes containing this sort of carbon ligand.[29]

As expected, the LUMO in both complexes is exclusively located at the bpy ligand tethered to the Re center.

Substitution of the hydrogen atoms of the alkynyl units in **3** by Pd(PH$_3$)$_2$Cl moieties in **5-H** perturbs slightly the electronic structure of the latter with respect to that of the former. In particular, MOs of the HOMO region are somewhat destabilized due to some interaction between π components of the triethynylbenzene moiety and the low-lying dπ FMOs of the palladium units in **5-H**. The orbital 1a″ of **3**, exclusively localized on the arylacetylide unit, is the most affected and becomes the HOMO−1 (3a″) of **5-H** with 12% Pd character. The energy destabilization of the HOMO region in **5-H** with respect to that of complex **3** leads to a smaller HOMO−LUMO gap in the former (0.95 vs 1.13 eV).

The Mulliken atomic net charges computed for **3** and **5-H** are given in Figure 5. An increase of the electronic density of the Re-alkynyl moiety is calculated upon substitution of the hydrogen atoms of the alkynyl ligands by Pd(PH$_3$)$_2$Cl moieties. The Re center is more electron-rich, gaining 0.27 electron. This reflects the stronger electron-donating ability of the Cl(PH$_3$)$_2$PdC≡C fragment with respect to HC≡C.

The electronic absorption spectra of **1**−**5** in THF show intense absorption bands at ca. 410−430 nm, with extinction coefficients on the order of 10^3 dm^3 mol^{-1} cm^{-1}. Table 3 summarizes the electronic absorption data of the complexes. The higher energy absorption bands at ca. 284−372 nm, which are also found in the free bipyridine and alkynyl ligands, are assigned as π → π* intraligand transitions of bipyridine and the alkynyl ligands. With reference to previous spectroscopic work on rhenium(I) diimine systems,[26] the intense low-energy absorptions at ca. 410−430 nm for **1**−**5** are tentatively assigned as the dπ(Re) → π*(diimine) metal-to-ligand charge transfer (MLCT) transition, probably with some mixing of an alkynyl-to-diimine [π(C≡C) → π*(diimine)] ligand-to-ligand charge transfer (LLCT) character. This is also supported by DFT calculations on complex **3** and the hydrogen-substituted model complex **5-H**, which show a LUMO of bpy π* character and HOMOs of rhenium and/or alkynyl character (see above). The occurrence of the MLCT absorption band of **1**−**5** at lower energies than that of their related precursor complexes, [Re(CO)$_3$(N^N)Cl], is suggestive of the higher-lying orbital energy of the dπ(Re) orbital in the alkynyl complexes, as a result of the better σ- and π-electron-donating abilities of the alkynyl ligand than the chloro counterpart, which renders the Re(I) center more electron-rich.

With different diimine ligands, a trend in the low-energy absorption was observed. The higher MLCT absorption energies of **1** (408 nm) and **2** (408 nm) than that of **3** (418 nm) are consistent with the higher π* orbital energies of ᵗBu$_2$bpy and Me$_2$bpy than bpy as a result of its poorer π-accepting abilities derived from the presence of the more electron-rich *tert*-butyl and methyl substituents on the bipyridine ligands. Similarly, the

(29) See for example: (a) Weyland, T.; Costuas, K.; Toupet, L.; Halet, J.-F.; Lapinte, C. *Organometallics* **2000**, *19*, 4228, and references therein. (b) Wong, K. M.-C.; Lam, S. C.-F.; Ko, C.-C.; Zhu, N.; Yam, V. W.-W.; Roué, S.; Lapinte, C.; Fathallah, S.; Costuas, K.; Kahlal, S.; Halet, J.-F. *Inorg. Chem.* **2003**, *42*, 7086.
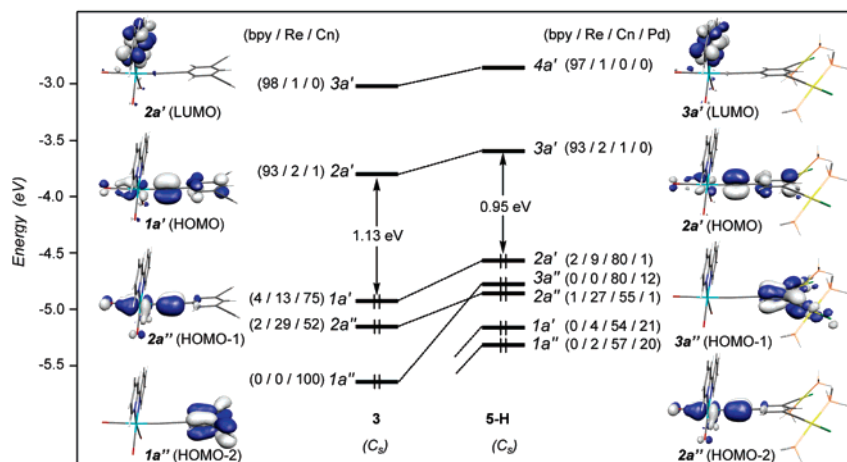
Figure 4. DFT MO diagrams of complex **3** (left) and the hydrogen-substituted model complex **5-H** (right). The bpy/Re/ carbon spacer (**3**) and bpy/Re/carbon spacer/Pd (**5-H**) percentage contributions of the MOs are given in parentheses.
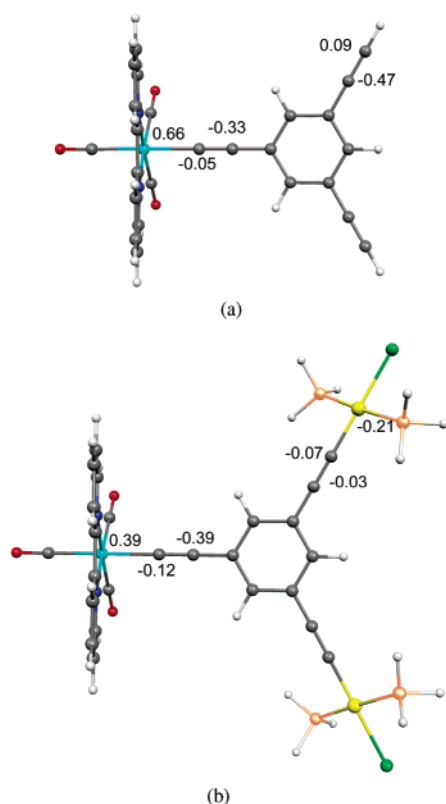
Figure 5. Pertinent Mulliken atomic net charges for complex **3** (a) and the hydrogen-substituted model complex **5-H** (b).

MLCT absorption energy of **4** (416 nm) is higher than that of **5** (426 nm) for the same reason.

On the other hand, a red shift in the absorption energy on going from **2** (408 nm) to **4** (416 nm) was observed upon the incorporation of palladium(II) metal centers into the rhenium alkynyl unit. This is consistent with the stronger electron-donating ability of Cl(PEt₃)₂-PdC≡C than that of HC≡C, which renders the Re(I) center more electron-rich and raises the dπ(Re) orbital energy, leading to a lower MLCT energy. A similar trend of MLCT absorption energy is also observed in the related analogues, in which **3** (418 nm) is found to show a higher MLCT absorption energy than that of **5** (426 nm). This is in agreement with DFT calculations carried out on complex **3** and the hydrogen-substituted model

complex **5-H**, which indicate a smaller HOMO−LUMO gap for the complexes containing palladium centers (see above).

Upon photoexcitation of **1**−**5** at $\lambda > 400$ nm, strong orange luminescence was observed both in the solid state and in fluid solutions at room temperature, attributed to the ³MLCT phosphorescence. The MLCT emission energies of **1** (625 nm) and **2** (625 nm) in tetrahydrofuran are higher than that of the corresponding analogue **3** (636 nm). This could be ascribed to the electron-donating effect of the *tert*-butyl or methyl substituents on the bipyridine ligand, which would raise the π^* orbital energies of ᵗBu₂bpy or Me₂bpy over that of bpy. Similarly, the MLCT emission energy of **4** (628 nm) is higher than that of **5** (639 nm). The rhenium(I) alkynyl complexes **1** and **2** with *tert*-butyl and methyl substituents on the bipyridine ligands, respectively, show MLCT emission energies similar to the electron-donating abilities of the *tert*-butyl and methyl groups, and hence the π-accepting abilities of ᵗBu₂bpy and Me₂-bpy are quite similar.

With different alkynyl ligands, a trend in the MLCT emission energy was also observed. Although the difference in the emission energies is small, it could be suggested that the slightly higher MLCT emission energy in **2** (625 nm) compared to **4** (628 nm) and also **3** (636 nm) compared to **5** (639 nm) is consistent with the trends observed in their electronic absorption studies. Indeed, similar but more obvious trends can be observed in the solid state at room temperature, as shown in Figure 6.

The cyclic voltammograms of **1**−**5** in acetonitrile (0.1 mol dm⁻³ ⁿBu₄NPF₆) display an irreversible oxidation wave at ca. +1.00 to +1.08 V, a quasi-reversible oxidation couple at ca. +1.75 to +1.82 V, and a quasi-reversible reduction couple at ca. −1.43 to −1.52 V vs SCE. An additional irreversible oxidation wave at ca. +1.40 V vs SCE was observed in the heterometallic complexes **4** and **5**. The electrochemical data are summarized in Table 4.

With reference to electrochemical studies on other related rhenium(I) diimine complexes,[26a,b] the first oxidation wave that occurred at ca. +1.0 to 1.1 V vs SCE was tentatively assigned as a Re(I) to Re(II) oxidation. All the complexes **1**−**5** showed a less positive potential

Table 3. Electronic Absorption and Emission Data for 1–5

complex	electronic absorption λ_{max}/nm (ϵ/dm^{3}mol^{-1}cm^{-1})[a]	emission medium (T/K)	λ_{em}/nm (τ_o/μs)
1	240 (51640), 294 (39680), 334 sh (12100), 408 (2840)	THF (298)	625 (<0.1)
		solid (298)	570 (0.26)
		solid (77)	573 (0.36, 0.21)[b]
		EtOH–MeOH glass (4:1 v/v) (77)	538 (2.56, 0.70)[b]
2	244 (52540), 294 (41180), 334 sh (12940), 408 (3020)	THF (298)	625 (<0.1)
		solid (298)	573 (0.20)
		solid (77)	559 (0.38)
		EtOH–MeOH glass (4:1 v/v) (77)	555 (3.36, 1.00)[b]
3	252 (30410), 294 (32010), 332 sh (12740), 418 (2590)	THF (298)	636 (<0.1)
		solid (298)	568 (0.28)
		solid (77)	564 (1.25, 0.22)[b]
		EtOH–MeOH glass (4:1 v/v) (77)	568 (3.27, 0.70)[b]
4	236 (57080), 284 (103890), 336 sh (16240), 416 (2250)	THF (298)	628 (<0.1)
		solid (298)	600 (<0.1)
		solid (77)	589 (0.73)
		EtOH–MeOH glass (4:1 v/v) (77)	546 (4.39, 0.73)[b]
5	238 (78150), 284 (99590), 334 sh (21590), 426 (2050)	THF (298)	639 (<0.1)
		solid (298)	598 (0.26)
		solid (77)	594 (0.62)
		EtOH–MeOH glass (4:1 v/v) (77)	565 (3.13, 0.78)[b]

[a] In THF at 298 K. [b] Double exponential decay.
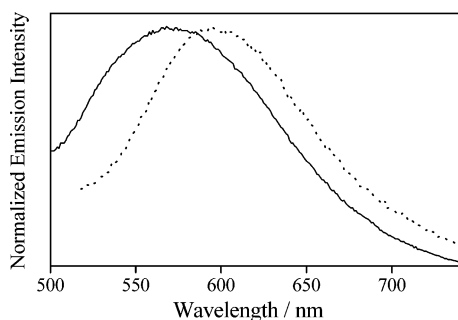
Figure 6. Solid-state emission spectra of [1,3-(HC≡C)$_2$-5-{(Me$_2$bpy)(CO)$_3$ReC≡C}C$_6$H$_3$] (**2**) (—) and [1,3-{Cl(PEt$_3$)$_2$-PdC≡C}$_2$-5-{(Me$_2$bpy)(CO)$_3$ReC≡C}C$_6$H$_3$] (**4**) (···) at room temperature.

Table 4. Electrochemical Data for 1–5

complex[a]	$E_{1/2}$[b]/V vs SCE (ΔE_p/mV)	
	oxidation	reduction
1	+1.06[c]	−1.52 (98)
	+1.80 (102)	
2	+1.05[c]	−1.52 (93)
	+1.78 (100)	
3	+1.08[c]	−1.44 (85)
	+1.82 (131)	
4	+1.00[c]	−1.52 (84)
	+1.38,[c] +1.75 (131)	
5	+1.03[c]	−1.43 (77)
	+1.40,[c] +1.81 (104)	

[a] In acetonitrile (0.1 mol dm^{-3} ^{n}Bu$_4$NPF$_6$). Working electrode: glassy carbon; ΔE_p of Fc$^+$/Fc ranges from 62 to 64 mV; scan rate, 100 mV s^{-1}. [b] $E_{1/2} = (E_{pa} + E_{pc})/2$; E_{pa} and E_{pc} are the anodic and cathodic peak potentials, respectively. $\Delta E_p = |E_{pa} - E_{pc}|$. [c] Irreversible oxidation wave. The potential refers to E_{pa}, which is the anodic peak potential.

for their first oxidation wave than their chloro counterparts, [Re(CO)$_3$(N^N)Cl], consistent with the better σ- and π-donating ability of the alkynyl ligand than the chloro group, which would render the rhenium(I) metal center more electron-rich and hence increased its ease of oxidation. With the same diimine ligand, **4** (+1.00 V vs SCE) and **5** (+1.03 V vs SCE) showed a slightly less positive potential for their first oxidation wave than their corresponding analogues, **2** (+1.05 V vs SCE) and

3 (+1.08 V vs SCE), respectively, suggestive of a slight increase in the electron-donating ability of the alkynyl ligand upon incorporation of the Pd(PEt$_3$)$_2$Cl moieties, which renders the Re(I) center slightly easier to oxidize. This is supported by DFT calculations that show HOMOs higher in energy in the case of the palladium-substituted complex. The relatively small shifts in the oxidation potential upon changing the electron-richness of the alkynyl ligands are supportive of a metal-centered oxidation rather than an alkynyl ligand-centered one, which otherwise would give rise to a more obvious change in the oxidation potential.

The oxidation wave that occurred at ca. +1.80 V vs SCE was found to be relatively insensitive to the nature of the alkynyl ligand but to vary with the nature of the diimine ligand. An EC mechanism was proposed for this oxidation wave,[30] in which a weakening of the metal–carbon bond between the rhenium center and the 1,3,5-triethynylbenzene ligand occurred after the first oxidation. This resulted in the loss of an alkynyl radical to give the coordinative unsaturated intermediate [Re-(CO)$_3$(N^N)]$^+$, which then readily picked up an acetonitrile molecule from the solvent to form the corresponding solvento complex, [Re(CO)$_3$(N^N)(MeCN)]$^+$. Therefore, this oxidation process of the rhenium(I) alkynyl complexes **1–5** was tentatively assigned as the oxidation of Re(I) to Re(II) of the corresponding solvento analogues, [Re(CO)$_3$(N^N)(MeCN)]$^+$, in acetonitrile. The observation that [1,3-(RC≡C)$_2$-5-{(Me$_2$bpy)(CO)$_3$Re-C≡C}C$_6$H$_3$] (R = H, **2**, or Pd(PEt$_3$)$_2$Cl, **4**) showed a less positive potential for this oxidation wave than their corresponding counterparts, [1,3-(RC≡C)$_2$-5-{(bpy)-(CO)$_3$ReC≡C}C$_6$H$_3$] (R = H, **3**, and Pd(PEt$_3$)$_2$Cl, **5**), respectively, is in line with the presence of the more electron-rich and less π-accepting Me$_2$bpy ligand, which would make the Re(I) in [Re(CO)$_3$(Me$_2$bpy)(MeCN)]$^+$ more easily to oxidize than that in [Re(CO)$_3$(bpy)-(MeCN)]$^+$. Complexes **1** (+1.06 V vs SCE) and **2** (+1.05 V vs SCE) showed similar oxidation potentials for this

(30) (a) Breikss, A. I.; Abruna, H. D. *J. Electroanal. Chem.* **1986**, *201*, 347. (b) Lau, V. C. Y. Ph.D. Thesis, The University of Hong Kong, 1997.

oxidation wave, consistent with the similar electron-donating ability of the methyl and *tert*-butyl groups.

An additional irreversible oxidation wave at ca. +1.40 V vs SCE for the heterometallic complexes **4** and **5** was tentatively assigned as Pd(II) metal-centered oxidation. The observation that complexes **4** and **5** show a less positive potential than the *trans*-[Pd(PEt$_3$)$_2$Cl$_2$] precursor (+1.52 V vs SCE) is consistent with the better σ-donating ability of the alkynyl moiety than the chloro group, which would render the palladium(II) metal center more electron-rich and hence increases its ease of oxidation. However, the possible involvement of a 1,3,5-triethynylbenzene ligand-centered oxidation cannot be completely excluded since the free ligand also shows an irreversible oxidation wave at ca. +1.22 V vs SCE. A similar result was also found in the palladium-(II) branched alkynyl complexes.[31]

The quasi-reversible reduction couple, which was found to vary with the nature of the diimine ligand, was tentatively assigned as a bipyridyl ligand-centered reduction. Indeed, DFT calculations on the monoanion of **3** and **5-H** indicate that the added unpaired electron is localized on the bpy ligand. The observation that **1** (−1.52 V vs SCE) and **2** (−1.52 V vs SCE) showed a more negative reduction potential than **3** (−1.44 V vs SCE) is in line with the attachment of the electron-donating *tert*-butyl or methyl substituents on the bipyridine ligand, which would render the bipyridine ligand more electron-rich and poorer π-accepting, thus decreasing its ease of reduction.

Conclusion

A series of luminescent mononuclear and heterometallic rhenium(I) complexes containing the hyperbranched 1,3,5-triethynylbenzene ligand have been successfully synthesized, and the X-ray crystal struc-tures of **2** and **5** have also been determined. Their photophysical and electrochemical properties have been studied. All complexes exhibit an intense low-energy absorption at ca. 410−430 nm, tentatively assigned as the [dπ(Re) → π*(diimine)] MLCT transition, probably with some mixing of an alkynyl-to-diimine [π(C≡C) → π*(diimine)] LLCT character. Such an assignment has been supported by DFT calculations. Red shifts in the absorption and emission energies were observed upon incorporation of the Cl(PEt$_3$)$_2$PdC≡C moiety.

Supporting Information Available: This material is available free of charge via the Internet at http://pubs.acs.org.

OM049696L

(31) Yam, V. W. W.; Tao, C. H. Unpublished results.